Electronic Supplementary Information (ESI)

Epitaxial growth of orthorhombic $NaTaO_3$ crystals on $SrTiO_3$ (100) surface by flux coating

Sayaka Suzuki,[a] Hajime Wagata,[a] Kunio Yubuta,[b] Shuji Oishi,[a] Katsuya Teshima[*,a,c]

[a] Department of Environmental Science and Technology, Faculty of Engineering, Shinshu University, 4-17-1 Wakasato, Nagano 380-8553, Japan

[b] Institute for Materials Research, Tohoku University, 2-1-1 Katahira, Aoba-ku, Sendai 980-8577, Japan

[c] Center for Energy and Environmental Science, Shinshu University, 4-17-1 Wakasato, Nagano 380-8553, Japan

E-mail: teshima@shinshu-u.ac.jp

**Corresponding Author: Katsuya Teshima*

Experimental

$NaTaO_3$ crystals were grown on a single-crystalline $SrTiO_3$ (100) substrate in a two-step process: sputter deposition of a tantalum oxide (TaO_x) thin film as a Ta source for $NaTaO_3$, and its subsequent conversion into $NaTaO_3$. First, a TaO_x thin film was deposited on the $SrTiO_3$ (100) substrate (10 × 10 × 0.5 mm^3, Shinkosha Co., Ltd.) by sputtering, using Ta (Furuya Metal Co., Ltd.) as a target and a simple magnetron sputtering system (JFC-1600, JEOL) under an Ar atmosphere. Next, a 2 M $NaNO_3$ solution was prepared using reagent-grade $NaNO_3$ powder (99.0%, Wako Pure Chemical Industries, Ltd.); 10 μL of this solution was placed on the $TaO_x/SrTiO_3$, which had been dry-cleaned and hydrophilized by irradiation under vacuum-ultraviolet light (λ = 172 nm) from a xenon excimer lamp (UER172-200, Ushio Inc.). The solution-coated $TaO_x/SrTiO_3$ was dried in an electric oven at 100 °C for 30 min. The substrates were placed in a Pt case and covered with an alumina plate. The Pt case was heated to 600 °C at a rate of 100 °C·min^{-1} in an infrared heating furnace and then naturally cooled to room temperature in the furnace without holding the temperature. The products were immersed in warm water to remove any residual $NaNO_3$.

The $TaO_x/SrTiO_3$ and $NaTaO_3/SrTiO_3$ samples were examined by field-emission scanning electron microscopy (FESEM; SU8000, Hitachi) and transmission electron microscopy (TEM; EM-002B, Topcon and JEM-2010, JEOL). The elemental composition was investigated using an X-ray photoelectron spectrometer (XPS; JPS-9010MX, JEOL), energy-dispersive X-ray spectrometer (EDS; attached to a transmission electron microscope/scanning transmission electron microscope (TEM/STEM; JEM-2800, JEOL)), and X-ray diffractometer (XRD; SmartLab and MiniflexII, Rigaku) with Cu-Kα radiation (λ = 0.154 nm). The samples for cross-sectional observations were prepared using a focused ion beam (FIB) system (JIB-4000, JEOL).

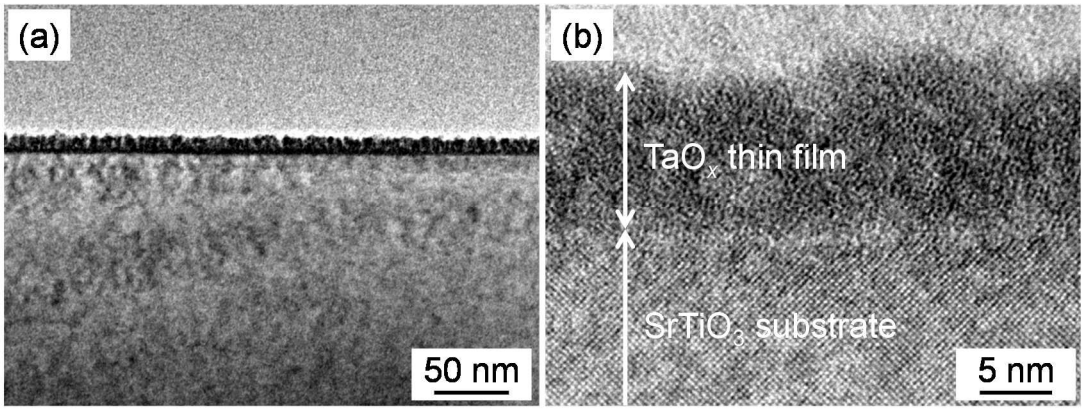

Figure S1. (a) Low- and (b) high-magnification cross-sectional TEM images of $TaO_x/SrTiO_3$.

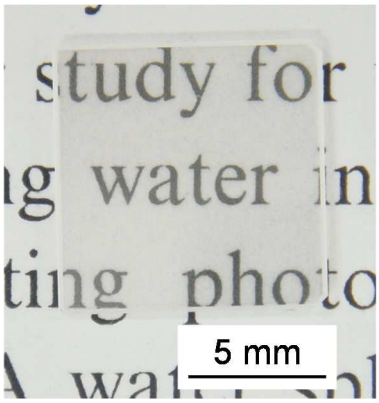

Figure S2. (a) Digital photograph of $TaO_x/SrTiO_3$.

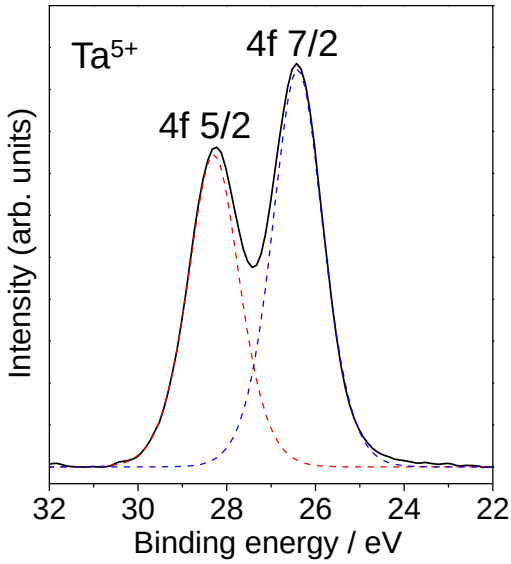

Figure S3. XPS spectra of TaO_x thin film deposited on an Al_2O_3 substrate. The TaO_x thin film was also deposited on a sapphire substrate at the same time with a $SrTiO_3$ substrate.

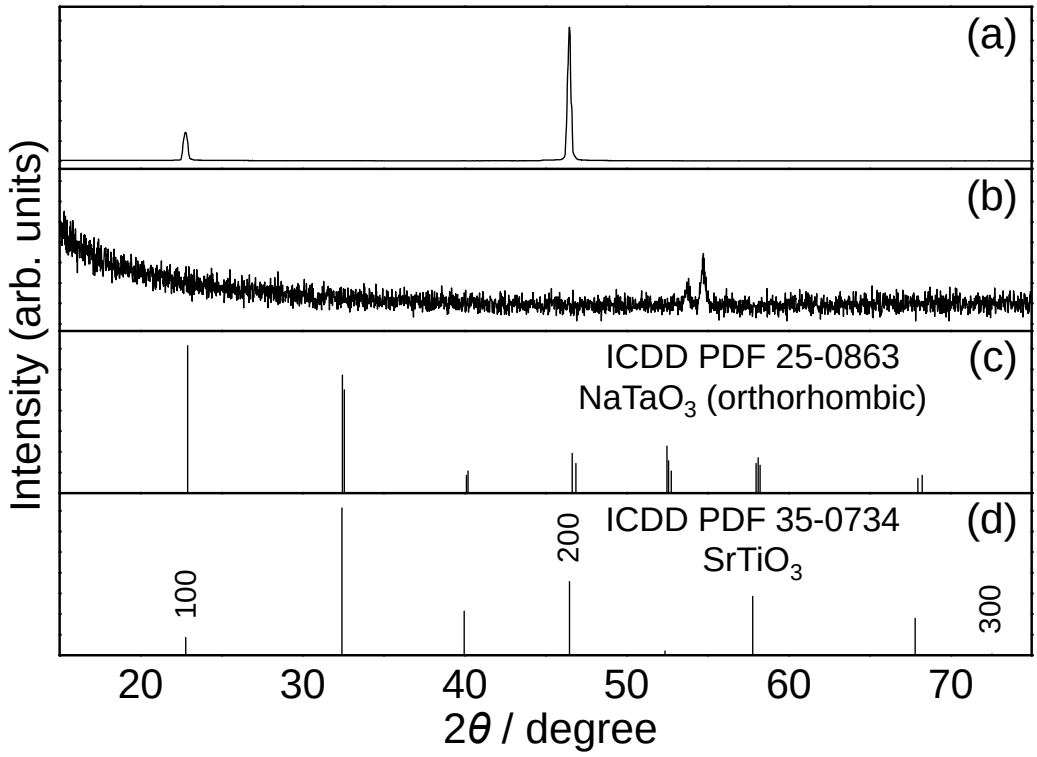

Figure S4. (a) XRD pattern obtained from $2\theta/\theta$ scan of $NaTaO_3/SrTiO_3$. (b) XRD pattern obtained from 2θ scan (ω = 1.0 °) of the $SrTiO_3$ substrate. XRD patterns of (c) $NaTaO_3$ (ICDD PDF data) and (d) $SrTiO_3$ (ICDD PDF data).

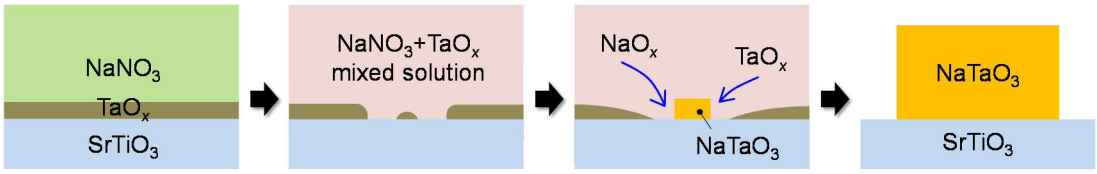

Figure S5. Illustrations of the growth mechanism of $NaTaO_3$ crystals from $NaNO_3$ and $TaO_x/SrTiO_3$. This figure shows the growth mechanism of epitaxially grown $NaTaO_3$ crystals rather than non-oriented ones.

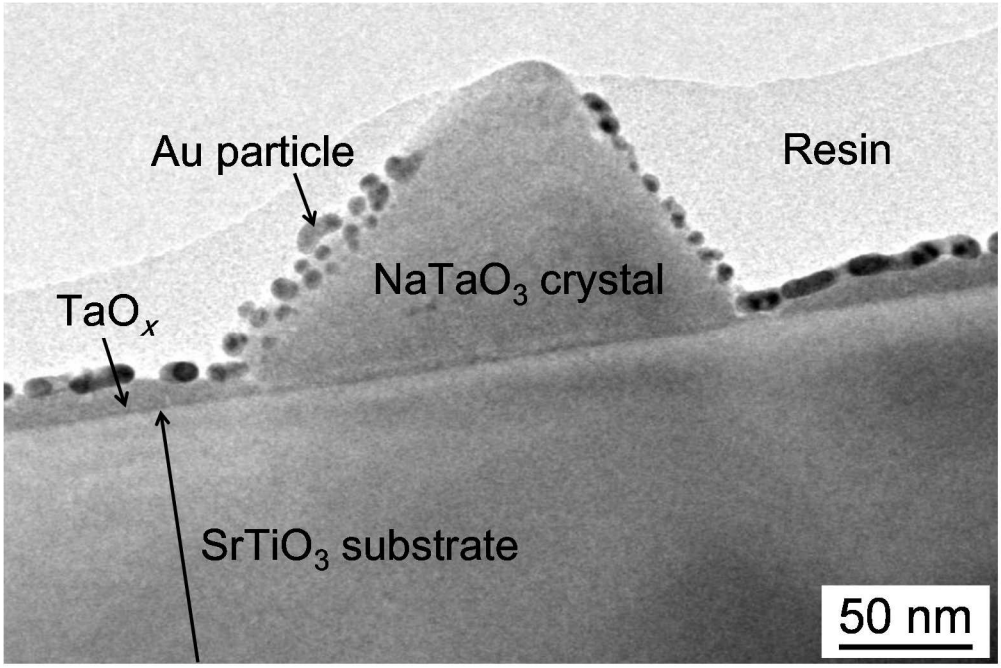

Figure S6. Cross-sectional TEM image of a disordered $NaTaO_3$ crystal grown on $SrTiO_3$ substrate. Au particles were deposited on $NaTaO_3/SrTiO_3$ before TEM observation in order to prevent the charging.

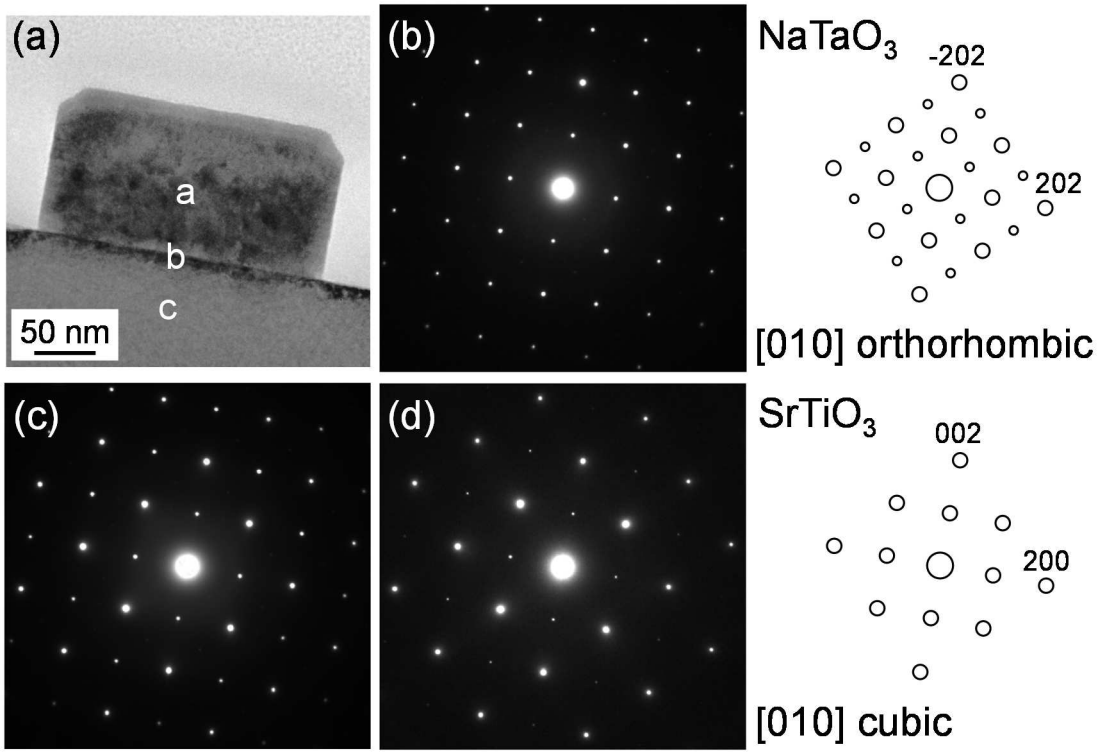

Figure S7. (a) Bright-field TEM image and (b−d) the corresponding SAED patterns of $NaTaO_3/SrTiO_3$. The incident electron beam was parallel to the [010] direction of $SrTiO_3$.

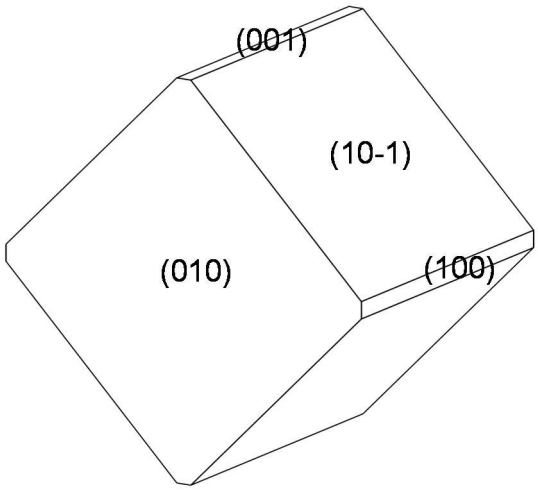

Figure S8. Schematic illustration of $NaTaO_3$ crystal bounded by {010}, {10-1}, {001}, and {100} faces.

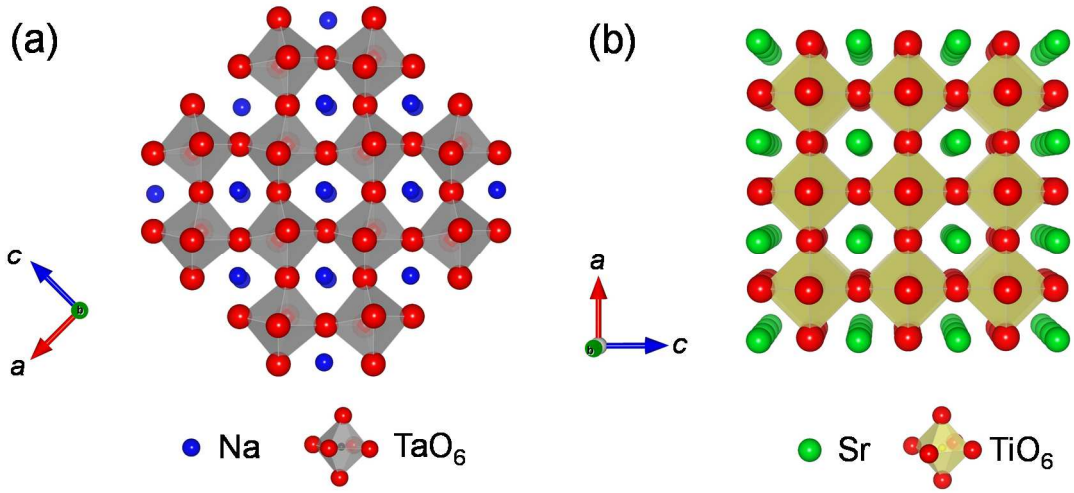

Figure S9. Schematic crystal structures of orthorhombic $NaTaO_3$ and cubic $SrTiO_3$.

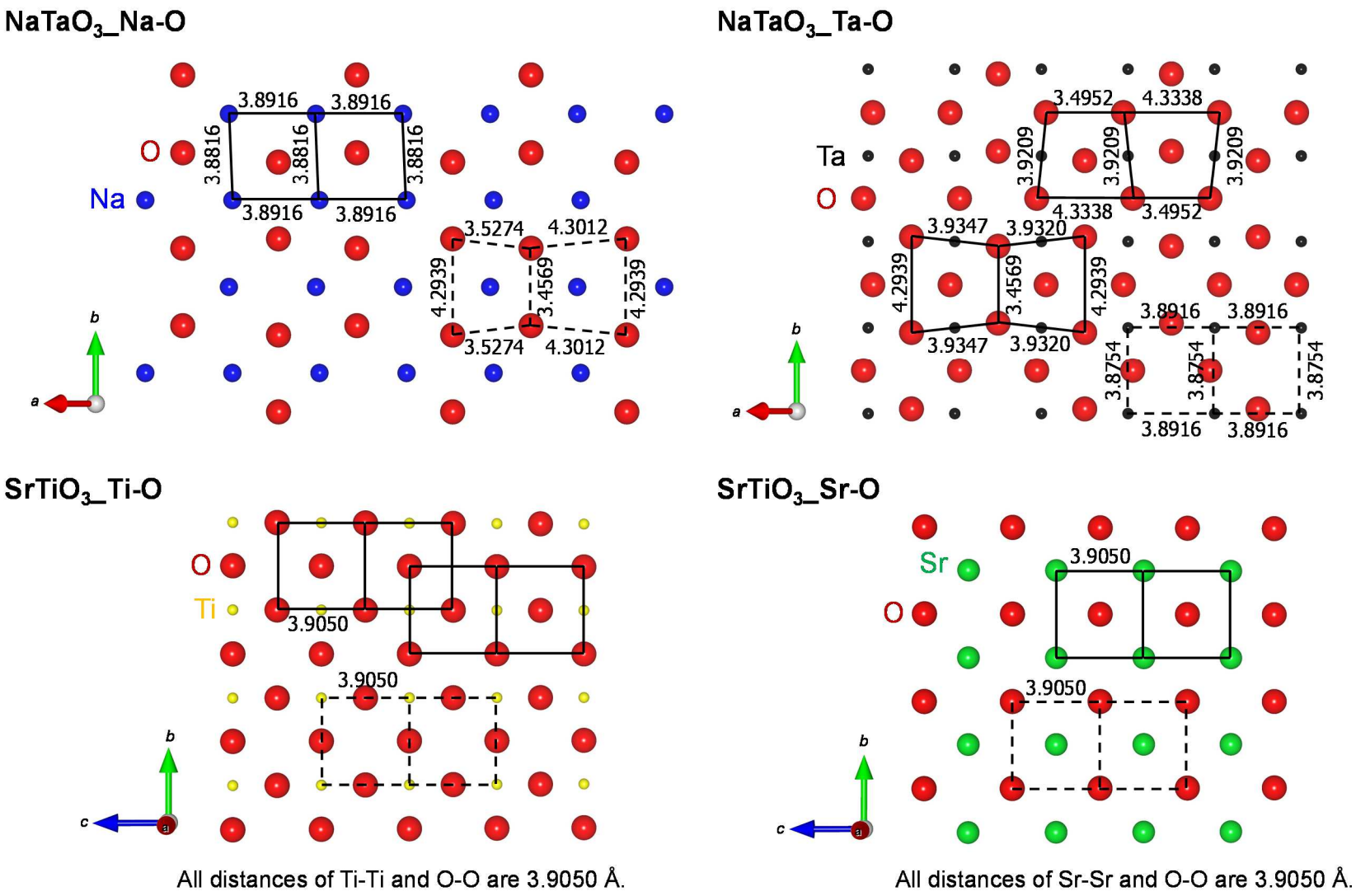

Figure S10. Schematic crystal structures of orthorhombic $NaTaO_3$ (10-1) face and cubic $SrTiO_3$ (100) face.